



# Experimental Study of a Novel Semi-Transparent Bi-Facial Agri-Voltaic System: Initial Results

Duncan McGraw<sup>1</sup> , Tonny Nyonga<sup>2</sup> , Laura Green<sup>2</sup> , Peter Vorobieff<sup>3</sup> ,  
David Hanson<sup>2,\*</sup> , Gowtham Mohan<sup>4</sup> , and Tito Busani<sup>1</sup> 

<sup>1</sup> Center for High Technology Materials, University of New Mexico, USA

<sup>2</sup> Department of Biology, University of New Mexico, USA

<sup>3</sup> Department of Mechanical Engineering, University of New Mexico, USA

<sup>4</sup> Cullen College of Engineering, University of Houston, USA

\*Correspondence: Tito Busani, busanit@unm.edu

**Abstract.** Solar (photovoltaic)-agriculture practices have experienced notable progress across several countries over the past few decades, creating a field widely known as agrivoltaics. This co-location practice has proved effective for certain crops that prefer partial shade like tomatoes, lettuce, and peppers, although it is less effective for crops needing more sun. Availability of natural sunlight with a specific spectral signature is necessary for agricultural practices as many plant species require an optimum-level and quality of sunlight for photosynthesis. The goal of this work is to model and validate ground-level irradiance for a semi-transparent bifacial solar collector equipped with a custom spectral reflector. By introducing intentional gaps between opaque solar cells, we hope to allow 50% of visible light to pass through the module. Additionally, this technology could reduce the soil temperature by 2° C, improve moisture retention, and enhance yield by providing partial solar radiation. In our model, we can calculate the total solar irradiance for the plants as a function of the cell distribution, material absorption, height of the panel and time of year with a spatial resolution of 0.0625 m<sup>2</sup>. When comparing theoretical estimates to experimental measurements of photosynthetically active radiation (PAR), we find a discrepancy of 32-48%, and a discrepancy of 19-38% after correction with TMY data.

**Keywords:** Agrivoltaics, Irradiance, Shading

## 1. Introduction

The concept of use of land for both photovoltaic power growth and agricultural development is often traced back to Adolf Goetzberger and Armin Zastrow's 1982 paper "On the Co-existence of Solar-Energy Conversion and Plant Cultivation". They outlined how 2 m tall elevated solar panels spaced apart by about 6 m would maintain uniform irradiance in the surrounding area [1]. As the state of the art evolved, researchers considered various parameters such as panel height, panel tilt and spacing between panels that could be customized across the thousands of agrivoltaic installations operating globally. In these installations, certain configurations provide several advantages to the crops, including improved crop yield, reduced soil temperature, higher soil moisture retention, and protection from extreme weather such as heavy rain, droughts, and hail [2,3,4]. Studies have also shown reduced module temperatures of up to 10° C for photovoltaic installations with plants growing beneath them compared to plain soil [5].

Given the linear trend between decrease in solar module temperature and increase in power produced from  $-20^{\circ}$  to  $50^{\circ}$  C, this would result in about a 2.7% increase in output power alone [6]. While these mutualistic benefits appear in some cases, there are still challenges that need to be addressed. The separation gap between solar panels, for one, introduces areas that are unavailable to produce electricity, resulting in a suboptimal collection of potentially available power. Additionally, the usage of standard opaque solar modules can lead to overshadowing in certain configurations, resulting in lower crop yields [7].

One way to address this challenge is to make photovoltaic panels semi-transparent, so that plants receive the benefits of partial shade while the collection area is increased to generate more electricity [8]. While there are many approaches in accomplishing this, they can generally be described as either non-selective or selective with respect to the wavelengths of incident light. Selective photovoltaic devices will absorb specified wavelengths while allowing others to transmit through the material, particularly photosynthetically active radiation (PAR) from 400 – 700 nm [9]. Non-selective photovoltaic devices will absorb a broad range of wavelengths. In the present work, we seek to utilize non-selective monocrystalline bifacial c-Si solar cells with intentional, even gaps between each other and a selective wavelength filtering layer to allow certain wavelengths to be transmitted to crops while filtering others out. There are several advantages to this strategy, starting with the use of the most ubiquitous type of solar cell, c-Si, low-cost in comparison to more expensive thin film technologies [10]. Additionally, the shading levels can be adjusted depending on the application by controlling the spacing of the cells.

Our proposed solar collector would incorporate thermoplastics in place of the typical components of PV modules with a goal of 50% of available visible light being transmitted to the plant canopy beneath. The inspiration for this comes from several factors including properties such as the ability to be melted down and remoulded almost indefinitely at relatively low temperatures [11], whereas glass requires specialized furnaces capable of heating to 1500-1600° C [12]. Some thermoplastics, such as PMMA, have high transparency (~90%) in the PAR wavelength range, are very flexible and have a low density compared with glass [13,14,15]. This warrants a comparison of the expected and measured PAR irradiance received by crops beneath an agrivoltaic installation of this design. In this work, we have built a simulation that can determine the ground-level irradiance of visible light at the plant canopy height for an agrivoltaic installation within MATLAB. Simultaneously, a test installation using PMMA sheets and aluminium tape was constructed as a mock agrivoltaic system with tomato, lettuce and kale plants growing underneath as described in Section 2. The physical installation also serves to validate the simulation that was developed through irradiance measurements conducted with a quantum light sensor, which is discussed in Section 3.

## 2. Materials and Methodology

### 2.1 System description and installation

For a preliminary test of an agrivoltaic panel installation elevated by support structures (Fig. 1), a set of partially transparent panels was installed on the roof of the University of New Mexico's Biology Department building. These panel prototypes used  $0.91 \times 1.92 \times 0.0024$  m OPTIX plexiglass sheets with stand-ins for the solar cells formed from aluminium tape to reflect or absorb the light that would be expected to reach the cell. Accordingly, while the setup could not produce electricity, it facilitated realistic shading conditions and was low-cost and easily reconfigurable.

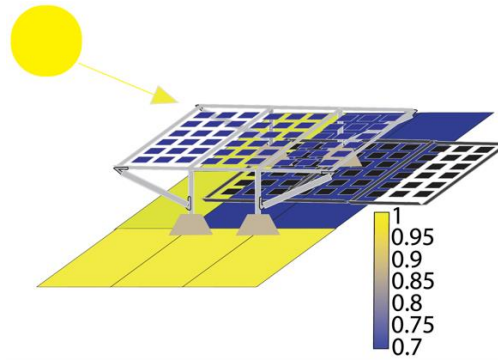


**Figure 1.** Diagram of semi-transparent bifacial modules and the fractional solar irradiance in area surrounding the panel for a single hour due to shading.

The plexiglass sheets were prepared for the construction by removing the protective film on both sides of the material, subdividing the panel into 18  $0.097 \text{ m}^2$  squares and marking the location of the mock cells within each square. Following this, aluminium tape was placed over the marked portion for the mock cell such that it was covered with no gaps. The frames were formed from  $4.13 \times 4.13 \text{ cm}$  galvanized steel slotted strut channels, six-hole three-side corner angle connectors, and  $10.2 \times 10.2 \times 30.6 \text{ cm}$  prefabricated-concrete strap pier blocks to hold the structure in place. The central frames were constructed by fastening four  $0.762 \text{ m}$  struts vertically to the concrete blocks with  $1.27 \text{ cm}$  or  $1.43 \text{ cm}$  bolts, then attaching a 3-side 6-hole corner connector to the top of the vertical strut. After this, two  $1.753 \text{ m}$  struts and two  $0.838 \text{ m}$  struts were secured to the corner connectors to form a rectangular shape. The plexiglass sheets were then placed on top to mark where  $1.27 \text{ cm}$  holes should be drilled to fasten them to the frame and once the holes were drilled, the sheets were mounted on top of the frame, as shown in Figure 2(a).

Following the completion of the frames, kale seeds were planted in raised beds; however, after several weeks, it became clear that the shading area from the panels would need to increase. To accomplish this while also reducing costs, a modification to the design was applied in which two additional panels with the same cell coverage percentage would be cantilevered off the central structure. Additional construction struts were placed along the length of the far side of the panels to distribute pressure more evenly. The additional panels were then added to each side of the frame with holes drilled for the bolts as well, as shown in Figure 2 (b).



**Figure 2.** (a) A photograph of solar panels stand-ins with the original design; (b) a photograph of 0% cell coverage cantilevered mock agrivoltaic installation and plants growing underneath.

## 2.2 Shading Simulation

To aid in the placement of crops with respect to the elevated panel of a given height and cell coverage percentage, a geometric shading simulation was developed within MATLAB. To begin, initial irradiance values were calculated. The key quantities calculated were the solar elevation angle  $\alpha(d, h)$  in radians, solar azimuth angle  $\theta(d, h)$  in radians, the air mass  $AM(d, h)$

and the direct beam irradiance  $I_D$  in  $\frac{W}{m^2}$  [16,17]. The referenced sources can be consulted for derivations of these parameters.

For each solar cell, the length of a shadow projected in the opposite direction of the sun's azimuth angle is computed for both axes of the plane formed by the ground, as given by the formulae

$$l_x(d, h) = \frac{a_{panel}}{\tan(\alpha(d, h))} \cos(\theta(d, h)) \quad (1)$$

and

$$l_y(d, h) = \frac{a_{panel}}{\tan(\alpha(d, h))} \sin(\theta(d, h)) \quad (2)$$

with  $a_{panel}$  being the height in m of the elevated solar panel in question. The coordinates of the shadow produced by each cell are then determined by adding this length to the coordinate of the cells' corners. To allow for a variety of cell coverage percentages, the number of cells was kept fixed, and the area of the cells was changed to match the desired percentage of the total panel area the user chooses to cover in cells.

For the rooftop installation, the mock panel was subdivided into 18 0.092903 m<sup>2</sup> squares, but the simulation was later expanded to consider the 72 cell "standard" solar panel. The simulation would then calculate the area covered by the mock cell within each square and obtain the side length. The coordinates of the corners of the cells are then computed by moving them such that the cell is centred. Once this is done, a grid of rectangles is formed for the area surrounding the panel and a series of conditions are applied to determine the fractional solar irradiance (FSI) received at each grid rectangle by calculating the shaded area and reducing the irradiance proportionally to the area covered at that hour of time. The fractional solar irradiance is defined as

$$FSI = \frac{I_{D,shaded}}{I_{D,unshaded}}, \quad (3)$$

where  $I_{D,shaded}$  indicates the intensity of light at the grid rectangle when accounting for transmission losses due to light obstruction and absorption and  $I_{D,unshaded}$  represents the unattenuated intensity of light at the ground. These fractional solar irradiances are then summed over the duration of the simulation such that a single two-dimensional array is produced representing the grid itself with fractional solar irradiance values ranging from 0 to 1. A colormap is then used to depict this, with a view of the simulated system being shown in Figure 1.

To estimate the usable light delivered to crops, one must consider how much of the total solar irradiance falls within the photosynthetically active radiation (PAR). In performing our own integration of the global spectral irradiance from the ASTM-G173 standard within the wavelength range of 400-700 nm, a value of 0.43 was obtained [18]. Following this, these values are then converted into units of photosynthetic photon flux density (PPFD) in  $\frac{\mu mol}{m^2 * s}$  using a conversion factor of  $1 J \approx 4.6 \mu mol$  as reported by Torres, et. al [19]. While these conversions are approximate, this should allow for a comparison between theoretical and measured values of irradiance.

## 2.3 Biological specimen preparation

Following the completion of the stand-in panel structures described in Section 2.1, three kinds of seeds, kale, tomatoes and lettuce, were planted in rectangular 10.2 x 10.2 cm<sup>2</sup> plastic pots, as shown in Figure 2(b). The seeds were placed in the centre of each pot, and a basin was used to water the plants from the bottom of the pots. Thirty plants were arranged in a rectangle under each installation in the area where the maximum amount of shading was predicted from the shading simulation. The plants were placed under the mock panels, as shown in Figure 2(b), starting on 6 April 2024 and will remain under them until the end of September 2024 with them being moved weekly by 4 cm to account for changes in the sun's altitude in the sky. Crop yield measurements as well as biological measurements of plant physiology will be the subject of a separate publication. Photosynthetically active radiation (PAR) measurements were taken at the canopy height of the leaves ~ 18 cm from the ground using a LI-COR photometer with a hemi-spherical quantum sensor facing upward. All the measurements were taken on full sun days at 7:30 am, 10:30 am, 1:30 pm and 4:30 pm within a 10 -15 minutes period to ensure consistency. In the case of the 50% covered panel, light measured in shaded spots was averaged with unshaded spots.

## 3. Results and Discussion

### 3.1 Shading simulation results for growing season

The simulation was customized for a 0.98 m panel height relative to the pots, 18 cells, a panel transmission of 92%, and a duration from April 1<sup>st</sup> to September 30<sup>th</sup>. The shading simulation demonstrates that the most shaded region of a 3x2 m<sup>2</sup> mock agrivoltaic system falling from 1 m N to 0.5 m S and from 0.5 m E to 0.5 m W, forming a region about 1.5 m<sup>2</sup> in area. The current resolution of the simulation produces 0.25 m x 0.25 m squares to aid in precise placement of biological replicants. Comparing the 50% and 100% cell coverage results (Figure 3(a,b)), one can see that the shape of the regions of minimum FSI are different. The 50% cell coverage plot appears to have shade concentrated along one horizontal and two vertical lines, while the 100% cell coverage plot has it within one block. This is likely due to the cell shadows falling in those locations during mid-day, significantly reducing the FSI.

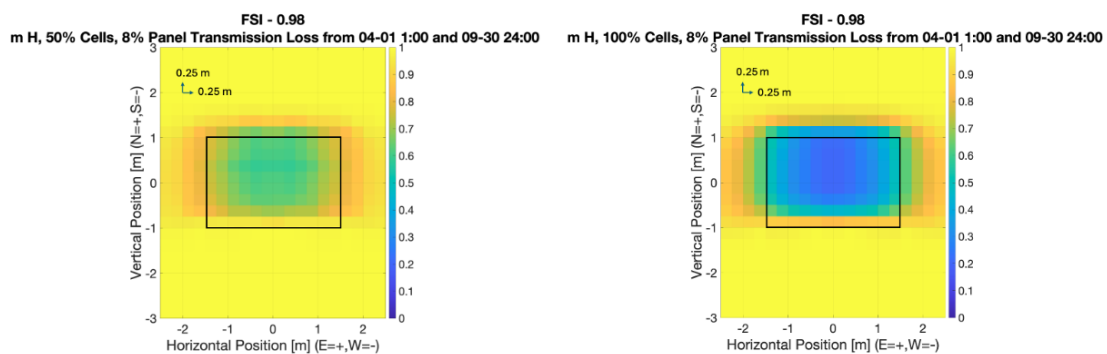


**Figure 3.** a colormap plot for expected fractional solar irradiance (FSI) in the area including and surrounding a 3x2 m panel, outline marked in black, for a) 50% coverage, b) 100% coverage.

### 3.2 Comparison with measured PPFD values

To give a closer comparison of the simulation's predicted solar irradiance and the PPFD measurements, the solar irradiance over a one-day period on 5 June 2024 when PPFD was also measured was calculated to be  $12.195 \frac{kW}{m^2}$ . The minimum FSI under the array was found to be

93.46% for the 0% cell coverage installation, 48.94% for the 50% cell coverage mock panels and 18.22% for the 100% cell coverage installation. The simulation accounts for absorption loss for light passing through the PMMA sheet, explaining why the 0% cell coverage installation has a value below 100%. From analysis of Typical Meteorological Data (TMY) data for the city of Albuquerque from 2022 [20], the full sun intensity measured was  $10.173 \pm 0.435 \frac{kW}{m^2}$ , which is 83.4% of the cloudless model.

For 0% cell coverage, the cloudless model obtained  $939.3 \frac{\mu mol}{s * m^2}$ , the TMY correction was  $783.6 \pm 33.5 \frac{\mu mol}{s * m^2}$  and the PPFD measurement was  $635.4 \pm 241.9 \frac{\mu mol}{s * m^2}$ . For 50% cell coverage, the cloudless model predicts a PPFD of  $491.9 \frac{\mu mol}{s * m^2}$ , the TMY correction is  $410.2 \pm 17.5 \frac{\mu mol}{s * m^2}$ , and the PPFD measurements were  $305.2 \pm 254.8 \frac{\mu mol}{s * m^2}$ . For 100% cell coverage, the cloudless model predicts  $183.12 \frac{\mu mol}{s * m^2}$ , the TMY correction gives  $152.8 \pm 6.5 \frac{\mu mol}{s * m^2}$ , and the PPFD measurements obtained  $95.4 \pm 83.9 \frac{\mu mol}{s * m^2}$ . These results are also presented in Table 1.

**Table 1.** a table comparing the minimum cloudless model PPFD value, minimum TMY correction PPFD value and PPFD measurement.

Percent Coverage	Cell	Cloudless Model	TMY Correction	PPFD Measurement
0%		$939.3 \frac{\mu mol}{s * m^2}$	$783.6 \pm 33.5 \frac{\mu mol}{s * m^2}$	$635.4 \pm 241.9 \frac{\mu mol}{s * m^2}$
50%		$538.4 \frac{\mu mol}{s * m^2}$	$449.1 \pm 19.2 \frac{\mu mol}{s * m^2}$	$305.2 \pm 254.8 \frac{\mu mol}{s * m^2}$
100%		$183.12 \frac{\mu mol}{s * m^2}$	$152.8 \pm 6.5 \frac{\mu mol}{s * m^2}$	$95.4 \pm 83.9 \frac{\mu mol}{s * m^2}$

While these measurements do fall within  $1\sigma$  of the TMY correction simulation values and  $2\sigma$  of the cloudless model, they do have rather high uncertainty. This is likely due to the data being collected for four hours of the day, making it unrepresentative of the temporal distribution of photosynthetically active radiation over a full day. One way to improve this methodology would be to collect less measurements but at more time intervals, which we hope to implement as the experiment progresses.

## 4. Conclusion

The field of agrivoltaics has developed significantly in the past 40 years, yet there are still obstacles in wider adoption of agrivoltaic installations. In general, there are two different kinds of agrivoltaic solar module designs, selective and non-selective, but there has yet to be one that incorporates intentional gaps in c-Si solar cells while also maximizing transmission of photosynthetically active radiation (PAR) to crops such that it draws upon the strength of both. To understand the effectiveness of a solar module with a certain cell coverage percentage, a customized geometric shading simulation was designed to ascertain the fractional solar irradiance in the area surrounding the elevated solar panel. Concurrently, a physical installation with mock solar panels mounted above crops was built such that shading simulation data would reveal the precise location of maximum shading and test crops could be grown there. Integrating over the growing season for Albuquerque (the beginning of April to the end of September), the region of maximum shading receives 48.94% of full sun for 50% cell coverage and 18.22% of full sun for 100% cell coverage. The calculated solar irradiances were found to be higher than experimentally measured results by 32-48%. When TMY data was incorporated, this deviation

was reduced to 19-38%, showing the simulation to be mostly accurate, but can be further improved with a better data collection methodology.

## Data availability statement

The data supporting these findings are available through the corresponding author, Tito Busani.

## Underlying and related material

The simulation scripts used in the production of this work are based in MATLAB and their working principles are described in depth in Section 2.2.

## Author contributions

**Duncan McGraw**: Conceptualization, Methodology, Software, Formal Analysis, Writing – Original Draft, Writing – Review and Editing, **Tonny Nyonga**: Conceptualization, Data Curation, Methodology, **Laura Green**: Conceptualization, Data Curation, Methodology, **Peter Vorobieff**: Conceptualization, Writing – Review and Editing, Funding acquisition, **Gowtham Mohan**: Conceptualization, Funding acquisition, **David Hanson**: Conceptualization, Funding acquisition, **Tito Busani**: Conceptualization, Writing – Review and Editing, Funding acquisition.

## Competing interests

The authors declare that they have no competing interests.

## Funding

We would like to thank the U.S. Department of Energy's Solar Energy Technologies Office (SETO) and the Minority Serving Institution STEM Research and Development Consortium (MSRDC) for funding this project.

## Acknowledgements

We would like to thank the UNM Departments of Mechanical Engineering, Biology and Electrical Engineering as well as the Center of High Technology Materials for their logistic support as well as Zadid Shifat, Henry Hao, Kirt Nakagawa, and Isaiah Deane for help in assembling the mock agrivoltaic structures, Trinity Griffus for help in collecting PAR measurements and the National Renewable Energy Laboratory for their TMY data.

## References

[1] Goetzberger, A, and Zastrow, A., "On the Coexistence of Solar-Energy Conversion and Plant Cultivation," *J. Sol. Energy*, vol.1, no.1, pp. 55-69, Jan. 1982, <https://doi.org/10.1080/01425918208909875>.

[2] Kumpanalaisatit, K., Setthapun, W., Sintuya, H., et al, "Current status of agrivoltaic systems and their benefits to energy, food, environment, the economy and society," *Sustain. Prod. Consum.*, vol.33, pp. 952–963, Sept. 2022, <https://doi.org/10.1016/j.spc.2022.08.013>.

- [3] Aroca-Delgado, R., Perez-Alonso, J., Callejon-Ferre, A.J., et. al, "Compatibility between Crops and Solar Panels: An Overview from Shading Systems", *Sustainability*, vol.10, no.743, pp. 1-19, Mar. 2018, <https://doi.org/10.3390/su10030743>.
- [4] Willockx, B., Reher, T., Lavaert, C., et. al., "Design and evaluation of an agrivoltaic system for a pear orchard", *App. Energy*, vol.353, Part B, no.122166, pp. 1-15, Oct. 2023, <https://doi.org/10.1016/j.apenergy.2023.122166>.
- [5] Williams, H. J., Hashad, K., Wang, H. M., et. al., "The potential of agrivoltaics to enhance solar farm cooling," *App. Energy*, vol.332, no.120478, pp. 1-11, Dec. 2022, <https://doi.org/10.1016/j.apenergy.2022.120478>.
- [6] Ebhota, W.S. and Tabakov, P.Y., "Influence of photovoltaic cell technologies and elevated temperature on photovoltaic system performance," *Ain Shams Eng. J.*, vol.14, no.101984, pp. 1-10, Oct. 2022, <https://doi.org/10.1016/j.asej.2022.101984>.
- [7] X.Y. Wolff, "Productivity of vegetable crops grown under shade in Hawaii", PhD thesis, University of Hawaii, 1988.
- [8] Gorjian, S., Bousi, E., Özdemir, Ö. E., et. al. "Progress and challenges of crop production and electricity generation in agrivoltaic systems using semi-transparent photovoltaic technology," *Renew. Sustain. Energy Rev.*, vol.158, no.112126, pp. 1-21, Apr. 2022, <http://dx.doi.org/10.1016/j.rser.2022.112126>.
- [9] Stallknecht, E. J., Herrera, C. K., Yang, C., et al., "Designing plant-transparent agrivoltaics", *Sci Rep*, vol.13, no.1903, pp. 1-14, Feb. 2023, <https://doi.org/10.1038/s41598-023-28484-5>.
- [10] Zotti, M., Mazzoleni, S., Mercaldo, L., et. al. "Testing the effect of semi-transparent spectrally selective thin film photovoltaics for agrivoltaic application: A multi-experimental and multi-specific approach", *Heliyon*, vol.10, no.42024, pp. 1-13, Feb. 2024, <https://doi.org/10.1016/j.heliyon.2024.e26323>.
- [11] Garcia, J. M. and Robertson, M. L., "The future of plastics recycling," *Science*, vol.358, no.6365, pp. 870–872, Nov. 2017, <https://doi.org/10.1126/science.aaq0324>.
- [12] Tapasa, K. and Jitwatcharakomol, T., "Thermodynamic calculation of exploited heat used in glass melting furnace," *Procedia Eng.*, vol.32, pp. 969 – 975, Mar. 2012, <https://doi.org/10.1016/j.proeng.2012.02.040>.
- [13] Chiromawa, N. L. and Ibrahim, K., "Effects of poly (methyl methacrylate) PMMA, film thickness in the Light Transmission through SiO<sub>2</sub> for Applications in Solar Cells Technology," *Int. J. Eng. Innov. Tech.*, vol.5, no.1, Jul. 2015, pp.125-131, <https://doi.org/10.17605/osf.io/r6svf>.
- [14] Ramanathan, S., Lin, Y.-C., Thirumurugan, S., et. al., "Poly(methyl methacrylate) in Orthopedics: Strategies, Challenges and Prospects in Bone Tissue Engineering," *Polym. J.*, vol. 16, no. 367, Jan. 2024, <https://doi.org/10.3390/polym16030367>.
- [15] Lobanov, S.S., Speziale, S., Winkler, B., et. al. "Electronic, Structural, and Mechanical Properties of SiO<sub>2</sub> Glass at High Pressure Inferred from its Refractive Index", *Phys. Rev. Lett.*, vol. 128, no. 077403, 2022, <https://doi.org/10.1103/PhysRevLett.128.077403>.
- [16] Luque, A. and Hegedus, S., "Energy Collected and Delivered by PV Modules" in *Handbook of Photovoltaic Science and Engineering*, 2<sup>nd</sup> ed. West Sussex, UK: JWS, 2011, ch.22, sec.2-3, pp.985-993.



[17] Laue, E. G., "The measurement of solar spectral irradiance at different terrestrial elevations". *Sol. Energy*, vol.13, no.1, pp.43-50, Apr. 1970. [https://doi.org/10.1016/0038-092X\(70\)90006-X](https://doi.org/10.1016/0038-092X(70)90006-X).

[18] Gueymard, C., "Parameterized Transmittance Model for Direct Beam and Circumsolar Spectral Irradiance," *Sol. Energy*, vol.71, no.5, pp. 325–346, Nov. 2001, [https://doi.org/10.1016/S0038-092X\(01\)00054-8](https://doi.org/10.1016/S0038-092X(01)00054-8).

[19] Torres, A. P. and Lopez, R. G., "Measuring Daily Light Integral in a Greenhouse," Department of Horticulture. Purdue University. 2010.

[20] National Renewable Energy Laboratory, Typical Metrological Year Data: 35.0882° N, 106.6519° W, National Solar Radiation Database. Version 3.2.2, 1998-2022, Accessed 18/05/2024.